Croatian Society for Materials Protection

Metalurgija/Metallurgy

Vol. 65 No. 4 / 2026

Study on the Transformation Behavior of Q550D Steel at Continuous Cooling Conditions

Han Weina, Guo Lili*, Liu Xinyue and Zhang Shikun

https://doi.org/10.64486/m.65.4.2

School of Liaoning Provincial Engineering Research Center for High-Value Utilization of Magnesite, Yingkou Institute of Technology，Yingkou 115014, China
hanweina@yku.edu.cn; guolili@yku.edu.cn; liuxinyue@yku.edu.cn; zhangshikun@126.com
* Correspondence: guolili@yku.edu.cn

Type of the Paper: Article
Received: December 23, 2025
Accepted: February 24, 2026

Abstract: Taking industrial 30 mm-thick Q550D steel as the research object, JMatPro software was used to simulate and calculate its key parameters, including thermodynamic phase diagram, TTT/CCT curves and mechanical properties. Meanwhile, static thermal simulation tests were conducted to simulate the heat treatment process under different cooling rates, and corresponding samples were prepared. Microstructure characterization and property tests were carried out using metallographic microscope, Vickers hardness tester and other equipment. Finally, the measured CCT curves were plotted and compared with the simulation results. The results show that the microstructure changes regularly with the cooling rate, and the final microstructure is lath martensite. The microhardness increases sharply at first and then tends to be stable with the increase of cooling rate. When the cooling rate exceeds 50℃/s, the microhardness stabilizes at 288-297HV, which is consistent with the variation law of the simulation results.

Keywords: Q550D steel, JMatPro; cooling rate; CCT; microhardness

1. Introduction

As a microalloyed low-carbon bainitic steel, Q550D steel integrates high strength, excellent low-temperature toughness and weldability, and is widely used in heavy steel structures, bridge engineering, construction machinery and other fields. With the development of industrial equipment toward extreme working conditions, higher requirements have been put forward for the performance stability and reliability of Q550D steel [1–4]. Li [5] et al. experimentally investigated the effect of cooling rate on the microstructure and properties of Q550 steel, confirming that an increased cooling rate can promote bainitic transformation, refine the microstructure, and thus enhance the material strength. Li [6] et al. conducted a study on the controlled rolling and controlled cooling process of Q550D steel, and found that the mixing ratio of bainite and ferrite can be precisely regulated by optimizing the cooling system, which provides an effective technical approach for improving the tensile properties of the material. Xu [7] et al. focused on the metal inert gas (MIG) welded joints of Q550D low-alloy high-strength steel and 6252 armor steel, systematically analyzed the microstructural and mechanical property characteristics of the weld zone, and provided a reference for the optimization of dissimilar steel welding processes

https://doi.org/10.64486/m.65.4.2

and the strength-toughness matching of welded joints. Yang [8] et al. adopted a combined method of numerical simulation and experimental verification to conduct an in-depth study on the preheating-free welding technology of Q550 low-alloy high-strength steel applied in hydraulic structural components, clarified the influence mechanism of process parameters on welding quality, and offered an important reference for the "simulation-verification" process development idea of this steel grade. In summary, existing research on Q550D steel mainly focuses on process optimization and performance improvement. The basic matching between strength and toughness is achieved through adjustments to processes such as thermomechanical control process (TMCP), welding process, or heat treatment process. As a core parameter of heat treatment, the cooling rate dominates the final mechanical properties of the material by regulating austenite phase transformation kinetics, altering grain size, phase composition, and microstructure morphology [9–14]. Although existing studies [5] have clarified the correlation between cooling process and the microstructure and properties of Q550D steel, there are still some deficiencies. Most studies focus on the effects of single process parameters such as cooling temperature and tempering system, and lack systematic exploration on the microstructure transformation law under continuous cooling rate gradient. In particular, the critical cooling rate and microstructure evolution details of the transition from granular bainite to lath bainite and martensite have not been clarified, which makes it difficult to accurately guide the refined regulation of process parameters. JMatPro software, relying on its mature thermodynamic models and extensively validated physical models, has been verified in the process simulation of metallic materials [15–18] which provides a reliable tool for predicting the phase transformation behavior of Q550D steel.

In this study, a dual-verification research approach of "simulation-experimentation" was adopted to investigate the microstructure evolution and property variation rules of Q550D steel within the cooling rate range of 1–100 °C/s. On the one hand, JMatPro simulations were performed to predict the critical phase transformation temperatures, phase composition ratios and property change trends in advance, which provides a scientific basis for the design of experimental schemes and reduces the blindness of experiments. On the other hand, static thermal simulation experiments were utilized to accurately reproduce the microstructure transformation during the actual cooling process. The phase transformation critical points were measured by the dilatometry method, and the experimentally determined continuous cooling transformation (CCT) curves were plotted combined with metallographic observations. Meanwhile, the microhardness under different cooling rates was systematically tested. Finally, a quantitative relationship among cooling rate, microstructure and properties was established. The reliability of the simulation results was verified by experimental data, and the model parameters were modified, thus making the research conclusions more credible. This study aims to fill the gap in the quantitative research on the CCT behavior of Q550D steel over a wide cooling rate range, clarify the regulation mechanism of cooling rate on microstructures such as bainite and martensite, and provide solid theoretical support for the precise optimization of heat treatment processes of Q550D steel. It is of great practical significance for promoting the application of high-performance materials in various engineering fields.

2. Experimental Materials and Research Methods

2.1. Experimental Materials

Industrial-grade Q550D steel with a thickness of 30 mm was selected as the experimental material. The chemical composition of the tested steel was analyzed using a SPECTROLAB M7 direct-reading spectrometer, and its main chemical components are presented in Table 1.

https://doi.org/10.64486/m.65.4.2

Table 1. Main chemical composition of Q550D steel (wt%)

C	Si	Mn	P	S	Al	Ti	Cr	Nb	B
0.089	0.26	1.53	0.015	0.0023	0.031	0.014	0.28	0.037	0.0004

2.2. Research Methods

JMatPro software was adopted for numerical simulation. The Thermodynamic Properties module was used to calculate the thermodynamic phase diagram of the tested steel, so as to clarify the equilibrium phase composition and phase transformation temperature. The Phase Transformations module was employed to plot the TTA, TTT and CCT curves, analyzing the evolution law of room-temperature microstructure under different cooling rates. Combined with the calculation results of phase transformation kinetics, the Mechanical Properties module was utilized to calculate the microhardness and tensile mechanical properties of the tested steel under different cooling rates, thus predicting the mechanical properties of the steel at varying cooling rates.

Static thermal simulation experiments were conducted on a Gleeble-3500 thermal simulation testing machine. The machined samples were cylindrical with dimensions of φ3 mm × 10 mm. According to the phase diagram characteristics of low-carbon low-alloy steel, the samples were heated to 930 °C at a rate of 10 °C/s. This austenitizing temperature was selected to ensure the complete dissolution of proeutectoid phases such as pearlite and ferrite, while avoiding abnormal growth of austenite grains caused by excessively high temperature, which would otherwise affect the subsequent transformed microstructure and properties. In accordance with the TG15-62/2:1-2023 standard, a holding time of 3 minutes was set to fully eliminate the internal temperature gradient of the samples and ensure a homogeneous austenite structure. Subsequently, the samples were cooled to room temperature at cooling rates of 1 °C/s, 10 °C/s, 20 °C/s, 30 °C/s, 40 °C/s, 50 °C/s, 70 °C/s, and 100 °C/s, respectively. During the experiments, the cooling process was precisely regulated by the closed-loop temperature control system of the Gleeble-3500 testing machine to maintain a linear and constant cooling rate throughout the entire cooling stage. The start and finish temperatures of phase transformation under different cooling rates were determined by recording the dilatation-temperature curves during cooling and in conjunction with the tangent method. The microstructures of the samples after continuous cooling transformation were observed using an Axioscope 5 optical microscope (OM). Microhardness tests were performed with a ZHV1 Vickers hardness tester under a load of 100 g and a dwelling time of 10 s. For each sample, measurements were taken at 5 different positions, and the average value was adopted as the final hardness value.

3. Simulation Results and Analysis

3.1. Simulation and Analysis of Thermodynamic Phase Diagram

The calculated thermodynamic phase diagram of Q550D steel is shown in Figure 1. As can be seen from Figure 1, the equilibrium phase diagram of Q550D steel consists of 11 distinct phase regions, including liquid phase, austenite, ferrite, MnS, $Ti_4C_2S_2$, a small amount of phosphide (M_3P), and various types of carbides (M(C,N), MB_2C_{32}, cementite, M_7C_3, $M_{23}C_6$). The liquidus temperature is 1517.6 °C, at which δ-ferrite begins to precipitate from the liquid phase. With the decrease of temperature, a peritectic reaction takes place. When the temperature drops to 1477.7 °C, the liquid phase disappears completely, and γ-austenite with a face-centered cubic (FCC) structure is formed, thus completing the transformation from liquid phase to solid phase. Subse-

https://doi.org/10.64486/m.65.4.2

quently, when the temperature decreases to approximately 1359.9 °C, a tiny amount of Mn-containing precipitate (MnS) begins to appear. In the temperature range of 1192.3 °C to 844.6 °C, trace amounts of $Ti_4C_2S_2$ start to form, and the content of $Ti_4C_2S_2$ reaches a peak of about 0.01 % at 844.6 °C. When the temperature drops to 126.5 °C, the MnS phase disappears completely. In contrast, γ-austenite begins to transform into low-temperature ferrite at 838.6 °C, and when the temperature decreases to 684.2 °C, austenite is completely converted into ferrite and a small amount of carbides. The equilibrium phase composition of Q550D steel at room temperature is mainly 98.3 % ferrite phase, along with a small amount of carbides (M (C,N), cementite, etc.), $Ti_4C_2S_2$ and phosphide M_3P.

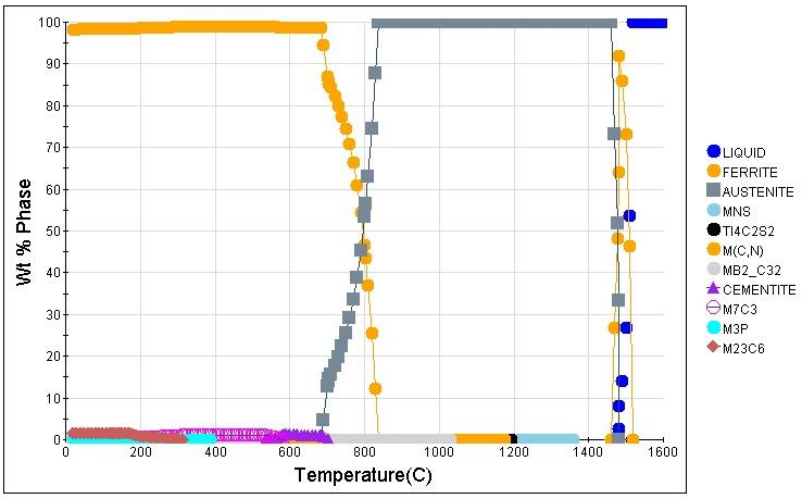

Figure 1. Thermodynamic phase diagram of Q550D steel calculated by JMatPro software

3.2. Simulation Results and Analysis of TTT Curve

Figure 2 shows the TTT curve calculated by JMatPro software. As can be seen from Figure 2, after the alloy is austenitized, the maximum precipitation temperatures of ferrite, pearlite and bainite during cooling are 838.7 °C, 697.8 °C and 603.6 °C, respectively. During these phase transformation processes, the "nose temperature" of pearlite is 607 °C, and undercooled austenite begins to precipitate pearlite after holding at this temperature for 77.8 s; the "nose temperature" of bainite is 517 °C, and undercooled austenite starts to precipitate bainite after holding at this temperature for 1.8 s; the martensite start temperature is 437.5 °C, the 50 % martensite transformation temperature (M_{50}) is 405.0 °C, and the 90 % martensite transformation temperature (M_{90}) is 329.5 °C.

The characteristics of the TTT curve indicate that the undercooled austenite of Q550D steel mainly undergoes ferrite-pearlite transformation in the medium-high temperature range 600–800 °C, bainite transformation dominates in the medium-low temperature range 500–600 °C, and martensite transformation occurs in the low temperature range (<437.5 °C), which is consistent with the phase transformation characteristics of low-carbon bainitic steel.

https://doi.org/10.64486/m.65.4.2

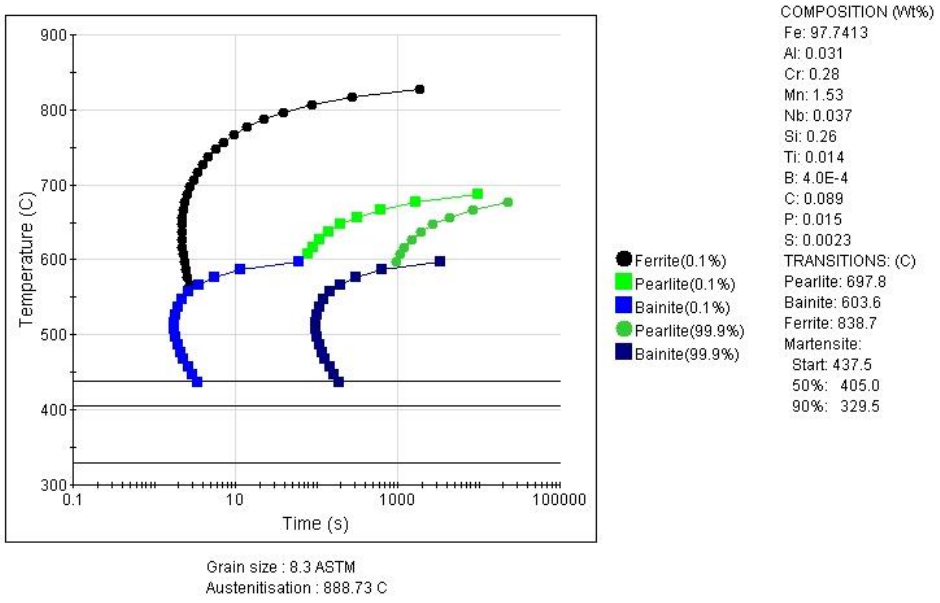

Figure 2. The TTT curve of Q550D steel calculated by JMatPro software

3.3. Simulation Results and Analysis of CCT Curve

Figure 3 shows the continuous cooling transformation curve of undercooled austenite in Q550D steel calculated by JMatPro software. As can be seen from Figure 3, during the continuous cooling process of Q550D steel, the minimum precipitation temperatures of ferrite, pearlite and bainite are 488.8 °C, 517.4 °C and 477.4 °C, respectively; the martensite start temperature (M_s) is 431.4 °C, and the martensite finish temperature (M_f) is 322.9 °C. When the quenching cooling rate is higher than 70 °C/s, the martensite content in the room-temperature microstructure reaches 99 %, which can be regarded as achieving a full martensite microstructure with the material fully quenched.

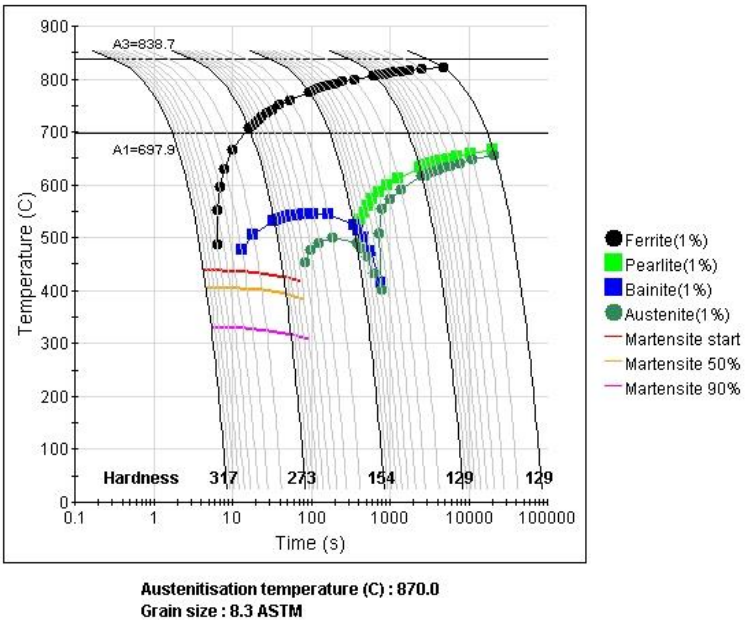

Figure 3. The CCT curve of Q550D steel calculated by JMatPro software

https://doi.org/10.64486/m.65.4.2

As can be seen from Figure 3, the room-temperature phase composition contents under different cooling rates are presented in Table 2. As can be seen from Table 2, when the cooling rate is 1 °C/s, the bainite content reaches 19.90 %. With a further increase in the cooling rate, the contents of ferrite and pearlite continue to decrease while the bainite content keeps rising. When the cooling rate increases to 10 °C/s, the martensite content is close to half of the total phase composition. At a cooling rate of 20 °C/s, the room-temperature microstructure is dominated by martensite, with the mass fraction of bainite accounting for only about 5 %, accompanied by a tiny amount of retained austenite. When the cooling rate increases to above 70 °C/s, the mass fraction of martensite is approximately 99 %, containing almost no bainite, and the content of retained austenite stabilizes at 0.01 %. It can be concluded that the increase in undercooling, i.e., the elevation of cooling rate, promotes the transformation of austenite to martensite. The proportion of martensite increases significantly with the rising cooling rate, while the bainite content shows a trend of first increasing and then decreasing.

Table 2. Room-temperature phase composition of Q550D steel at different cooling rates

Cooling rate/(°C·s⁻¹)	1	10	20	30	40	50	70	100
Ferrite/%	79.44	28.47	12.39	5.48	2.85	1.78	0.78	0.29
Pearlite/%	0.65							
Bainite/%	19.91	26.30	4.98	1.86	0.97	0.60	0.29	0.11
Austenite/%				0.01	0.01	0.01	0.01	0.01
Martensite/%		45.21	82.62	92.65	96.07	97.61	98.91	99.58

3.4. Simulation Results and Analysis of Mechanical Properties

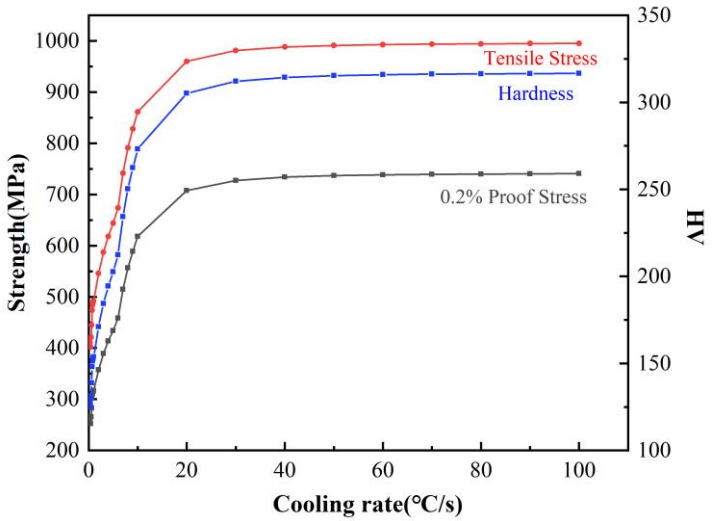

Figure 4. Mechanical properties of Q550D steel calculated by the JMatPro software

The simulation results of mechanical properties of Q550D steel are shown in Figure 4. As can be seen from Figure 4, the yield strength, tensile strength and microhardness exhibit the same variation trend with the cooling rate, which can be divided into two stages. In the first stage, when the cooling rate is less than 10 °C/s, the yield strength, tensile strength and microhardness increase almost linearly. This is because at low cooling rates,

https://doi.org/10.64486/m.65.4.2

the room -temperature microstructure is dominated by ferrite and a small amount of pearlite, which have relatively low hardness and strength. In the second stage, when the cooling rate exceeds 10 °C/s, the increasing rate of yield strength, tensile strength and microhardness gradually slows down. Especially when the cooling rate ranges from 30 °C/s to 100 °C/s, the three parameters basically tend to be stable. This is due to the fact that the core microstructure transformation in this stage is martensitic transformation, with a large number of dislocations and twins existing inside the material. Through the synergistic effect of dislocation strengthening, twin strengthening, and solid solution strengthening, the strength and hardness of the material reach a relatively high level.

4. Experimental Results and Analysis

4.1. Microstructure Analysis

The room-temperature microstructures of Q550D hot-rolled steel plates under different cooling rates are shown in Figure 5. As can be seen from Figure 5, with the increase of cooling rate, the microstructure transforms from ferrite + pearlite to bainite and martensite. When the cooling rate is 10 °C/s, a large amount of granular bainite appears in the microstructure, accounting for approximately 25.8 %. The ferrite content decreases, and its morphology gradually transforms from the original coarse polygonal shape to fine lath-like, while pearlite disappears completely. At a cooling rate of 20 °C/s, the proportion of bainite reaches 50 %, and its morphology transforms into lath-like, presenting a mixed state of granular and lath-like structures with further refined microstructure. When the cooling rate is 30 °C/s, martensite emerges in the microstructure, and the contents of both ferrite and bainite decrease. At a cooling rate of 40 °C/s, the microstructure is dominated by lath martensite, accounting for about 52.6 %, while the contents of ferrite and bainite continue to decrease, with the ferrite content only accounting for 25.4 %. When the cooling rate further increases to the range of 50 °C/s ~ 100 °C/s, the microstructure is almost entirely composed of martensite; moreover, with the increase of cooling rate, the size of martensite lath packets becomes smaller and smaller, and the microstructure refinement effect is significant. The mixed microstructure of granular bainite and lath bainite can achieve a balance between strength and toughness [19, 20].

4.2. CCT Curve Analysis

Based on the inflection points of the curves depicting variations of thermal expansion and temperature with time for Q550D steel under different cooling rates, which were obtained from thermal simulation tests, the tangent method was adopted to determine the phase transformation temperatures at different cooling rates. Combined with the metallographic microstructure morphology, the CCT curve of Q550D steel was constructed and is shown in Figure 6. As can be seen from the figure, with the increase of cooling rate, the initial phase transformation temperature decreases gradually. When the cooling rate reaches above 5 °C/s, bainite microstructure appears and gradually becomes the dominant phase; at this time, the microstructure is mainly composed of ferrite and bainite, and pearlite basically disappears. When the cooling rate increases to above 20 °C/s, martensite microstructure begins to form, and the room-temperature microstructure is mainly a mixture of martensite, bainite and ferrite. When the cooling rate exceeds 40 °C/s, ferrite disappears, and the microstructure is primarily a mixture of martensite and bainite. The overall variation trend of the phase transformation law reflected by the measured CCT curve is consistent with that simulated by JMatPro, which verifies the reliability of the simulation.

https://doi.org/10.64486/m.65.4.2

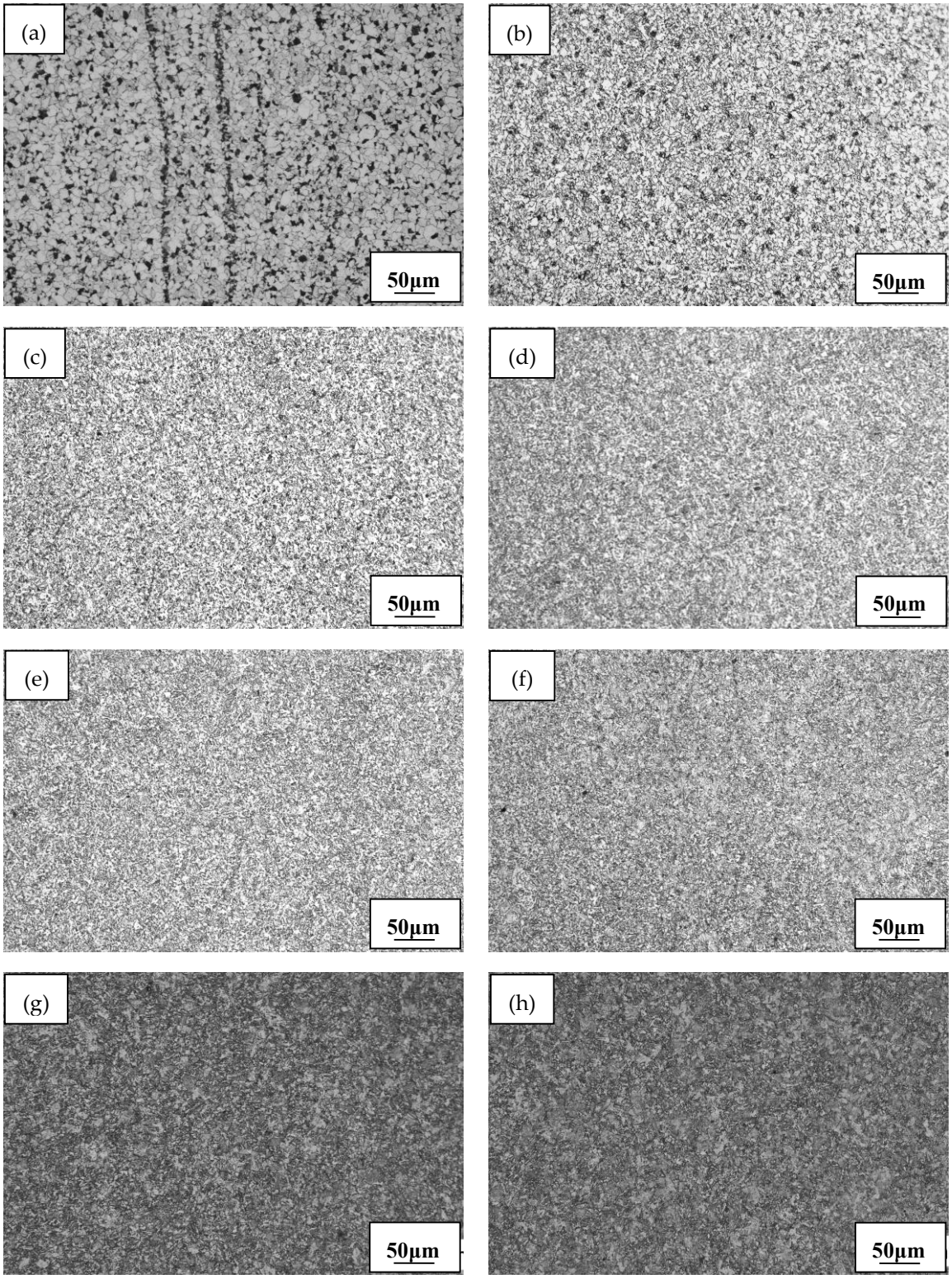

Figure 5. Room-temperature microstructure of Q550D steel under different cooling rates
(a) 1 °C/s; (b) 10 °C/s; (c) 20 °C/s; (d) 30°C/s; (e) 40 °C/s; (f) 50 °C/s; (g) 70 °C/s; (h) 100 °C/s

https://doi.org/10.64486/m.65.4.2

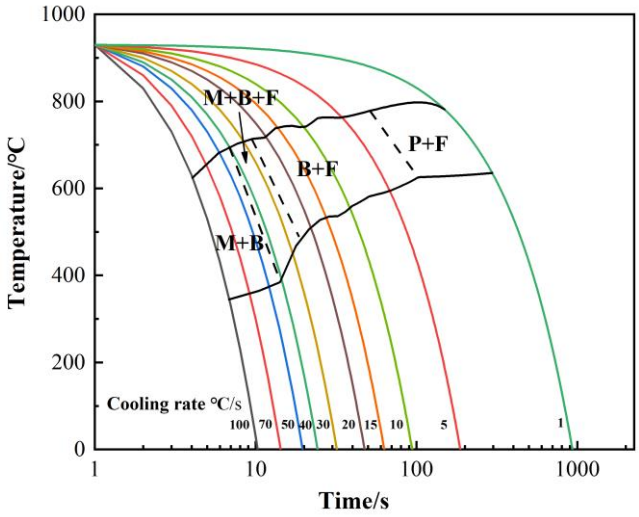

Figure 6. CCT diagrams of the Q550D steel

4.3. Microhardness Analysis

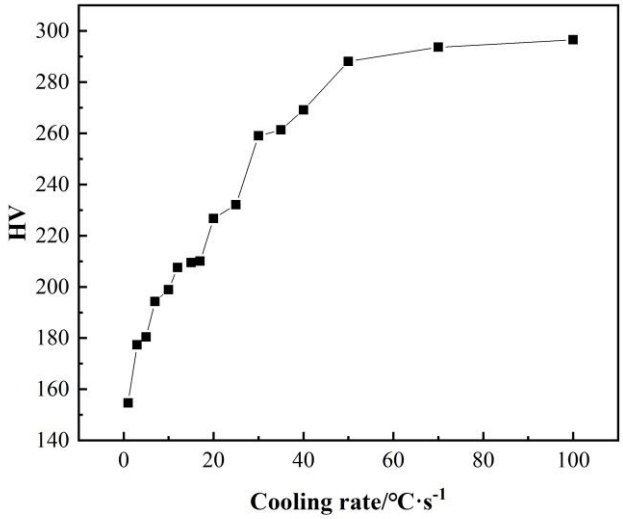

Figure 7. Microhardness of the Q550D steel under different cooling rates

Figure 7 shows the microhardness curve of Q550D steel under different cooling rates. As can be seen from Figure 7, the microhardness increases gradually with the rise of cooling rate. The main reason is that the increase in cooling rate refines the microstructure; meanwhile, the content of granular bainite increases gradually, and the strengthening effect of bainite leads to the improvement of hardness. With a further increase in cooling rate, the bainite content continues to rise and its morphology gradually transforms into lath bainite, which further refines the microstructure and thereby results in a continuous increase in microhardness. When the cooling rate exceeds 20 °C/s, martensite begins to appear in the microstructure. As the cooling rate increases further, the martensite content rises gradually while the contents of ferrite and bainite continue to decrease, and the phase

https://doi.org/10.64486/m.65.4.2

transformation strengthening effect of martensite further improves the hardness.

When the cooling rate reaches 100 °C/s, the microstructure is almost entirely composed of martensite, and the microhardness remains basically unchanged, with only a slight increase caused by the refinement of martensite lath packets. This is consistent with the rule that the mechanical properties tend to be stable in the simulation results. The measured microhardness stabilizes at 288–297 HV, corresponding to a tensile strength of approximately 685–725 MPa, which meets the application requirements of Q550D steel in the field of steel structures.

5. Conclusions

1. The thermodynamic phase diagram, TTT and CCT curves of Q550D steel were simulated and calculated by means of JMatPro software, and its phase transformation characteristic parameters were clarified: the liquidus temperature is 1517.6 °C, A1= 697.9 °C, A3= 838.7 °C, the martensite start temperature (M_s) is 431.4 °C, and the martensite finish temperature (M_f) is 322.9 °C. A full martensite microstructure can be obtained when the cooling rate is higher than 70 °C/s.
2. The microstructure of Q550D steel evolves regularly with the cooling rate. When the cooling rate ranges from 40 °C/s to 100 °C/s, a martensite-dominated microstructure is formed, and the martensite laths are refined with the increase of cooling rate. The microhardness increases sharply at first and then tends to be stable with the increase of cooling rate, which is highly consistent with the evolution law of the microstructure.
3. The overall trend of the measured CCT curve is consistent with that of the simulation results, which verifies the reliability of JMatPro software in predicting the phase transformation behavior of Q550D steel.

Acknowledgments: This work was funded by the Foundation of Liaoning Provincial Key Laboratory of Energy Storage and Utilization (CNNK202523), Liaoning Provincial Engineering Research Center for High-Value Utilization of Magnesite (LMNY2024020211), Youth Project of Yingkou Institute of Technology(QNL202423), Liaoning Provincial Department of Education Project (JYTMS20230062), the 2023 Liaoning Provincial Joint Fund Project Doctoral Scientific Research Initiation Project (2023-BSBA-308).

References

[1] F. P. Li, N. Li, X. L. Wang, and M. H. Liang, "Microstructure and Mechanical Properties of High Strength Low Alloy Steel Q550D," *Materials Science Forum*, vol. 6114, pp. 424–429, 2021, https://doi.org/10.4028/WWW.SCIENTIFIC.NET/MSF.1035.424.

[2] D. Ormston, V. Schwinn, and K. Hulka. "Development of Low Carbon Microalloyed Bainitic Steels for Structural PlateApplications," Materials Science Forum, vol. 531, no. 500-501, pp. 573-580, 2005, https://doi.org/10.4028/www.scientific.net/MSF.500-501.573

[3] X. L. He, C. J. Shang, X. M. Wang, S. W. Yang, and H. X. Hou. "The Development of Ultra-Fine High Performance Low Carbon Bainitic Structural Steel," Materials Science Forum, vols. 58, no. 539-543, pp. 4503-4508, 2007, https://doi.org/10.4028/www.scientific.net/MSF.539-543.4503

[4] B. Adamczyk-Cieślak, M. Koralnik, R. Kuziak, K. Majchrowicz, and J. Mizera. "Studies of Bainitic Steel for Rail Applications Based on Carbide-Free, Low-Alloy Steel," Metallurgical and Materials Transactions A, vol. 52, no. 12, pp. 5429-5442, 2021, https://doi.org/10.1007/S11661-021-06480-6

[5] F. Li, H. L. Yi, Z. Y. Liu, and G. D. Wang, "Influence of Cooling Rate on the Microstructures and Properties of Q550," *Applied Mechanics and Materials*, vol. 117–119, pp. 1705–1707, 2016, https://doi.org/10.4028/WWW.SCIENTIFIC.NET/AMM.117-119.1705.

[6] J. S. Li, Y. X. Liu, Y. Wang, and Z. Q. Dong, "Effect of Controlled Cold-Controlled Rolling Process on Properties of Q550D Steel Plate," *IOP Conference Series: Earth and Environmental Science*, vol. 692, no. 3, p. 032022, 2021,

 https://doi.org/10.64486/m.65.4.2

https://doi.org/10.1088/1755-1315/692/3/032022.

[7] X. Y. Xu, G. Wang, R. B. Zhang, and G. J. Zhang, "Microstructure and Mechanical Properties of MIG Welds between 6252 Armor Steel and Q550D HSLA Steel," *Materials*, vol. 15, no. 24, p. 9043, 2022, https://doi.org/10.3390/MA15249043.

[8] H. Yang, L. J. Wang, and F. Y. Hao, "Numerical Simulation and Test Study on Non-Preheating Welding Technology of HSLA Q550 Applied to Hydraulic Structures," *Advanced Materials Research*, vol. 546–547, pp. 110–114, 2012, https://doi.org/10.4028/www.scientific.net/AMR.546-547.110.

[9] Y. Yılmaz and M. F. Kılıçaslan, "Effect of cooling rate on the microstructure and magnetic properties of melt-spun CeFeB ribbons," *Journal of Magnetism and Magnetic Materials*, vol. 640, p. 173785, 2026, https://doi.org/10.1016/J.JMMM.2025.173785.

[10] I. Tripathy, M. Mallik, and S. B. Singh, "Effect of Austenitization and Cooling Rate on Pearlite Morphology and Kinetics of Near Eutectoid Steel: A Combined Experimental–Simulation Approach," *Journal of Phase Equilibria and Diffusion*, vol. 46, no. 4, pp. 1–18, 2025, https://doi.org/10.1007/S11669-025-01206-2.

[11] Y. L. Chen, X. J. Zhou, Y. Y. Jiang, and Q. X. Wang, "The influence law of cooling rate on microstructure and properties of low-carbon high-grade AF pipeline steel," *Int. J. of Microstructure and Materials Properties*, vol. 11, no. 5, pp. 373–382, 2016, https://doi.org/10.1504/IJMMP.2016.080700.

[12] X. F. Xiao, Y. Wang, C. S. Liu, F. Huang, H. Zhang, and H. W. Ni, "Effect of Cooling Rate and Sulfur Content on Inclusion Precipitation and Microstructure in X70 Pipeline Steel," *Steel Research International*, vol. 96, no. 10, pp. 534–549, 2025, https://doi.org/10.1002/SRIN.202500012.

[13] R. Bharadwaj, A. Sarkar, and B. Rakshe, "Effect of Cooling Rate on Phase Transformation Kinetics and Microstructure of Nb–Ti Microalloyed Low Carbon HSLA Steel," *Metallography, Microstructure, and Analysis*, vol. 11, no. 4, pp. 661–672, 2022, https://doi.org/10.1007/S13632-022-00864-9.

[14] M. Morawiec, A. Wojtacha, and M. Opiela, "Kinetics of Austenite Phase Transformations in Newly-Developed 0.17C-2Mn-1Si-0.2Mo Forging Steel with Ti and V Microadditions," *Materials*, vol. 14, no. 7, p. 1698, 2021, https://doi.org/10.3390/MA14071698.

[15] Y. H. Yu, J. X. Hou, P. Zhu, and J. L. Zhang, "Microstructure and properties of iron-based surfacing layer based on JmatPro software simulation calculation," *Vibroengineering Procedia*, vol. 50, pp. 180–186, 2023, https://doi.org/10.21595/VP.2023.23400.

[16] P. Yu, R. B. Song, W. M. Xiong, W. F. Huo, C. Wei, Z. J. Liu, and S. Qin, "Phase Transformation Law of Nb Microalloyed Steel at Different Cooling Rates," *Materials Science Forum*, vol. 6114, pp. 396–403, 2021, https://doi.org/10.4028/WWW.SCIENTIFIC.NET/MSF.1035.396.

[17] X. X. Geng, H. Wang, W. H. Xue, X. Song, H. L. Huang, M. Li, and G. Ma, "Modeling of CCT diagrams for tool steels using different machine learning techniques," *Computational Materials Science*, vol. 171, p. 109235, 2020, https://doi.org/10.1016/j.commatsci.2019.109235.

[18] R. C. Sun and G. B. Mi, "Influence of Alloying Elements Content on High Temperature Properties of Ti-V-Cr and Ti-Al-V Series Titanium Alloys: A JMatPro Program Calculation Study," *Journal of Physics: Conference Series*, vol. 2639, no. 1, 2023, https://doi.org/10.1088/1742-6596/2639/1/012019.

[19] Y. Zhang, Y. Cao, G. J. Huang, Y. Y. Wang, Q. L. Li, and J. He, "Influence of Martensite/Bainite Dual Phase-Content on the Mechanical Properties of EA4T High-Speed Axle Steel," *Materials (Basel, Switzerland)*, vol. 16, no. 13, 2023, https://doi.org/10.3390/MA16134657.

[20] B. S. Wang, N. N. Chen, Y. Cai, W. Guo, and M. Wang, "Effect of Microstructure on Impact Toughness and Fatigue Performance in Coarse-Grained Heat-Affected Zone of Bainitic Steel Welds," *Journal of Materials Engineering and Performance*, vol. 32, no. 8, pp. 3678–3689, 2022, https://doi.org/10.1007/S11665-022-07339-6.